Targeted vaccination against the bevacizumab binding site on VEGF using 3D-structured peptides elicits efficient antitumor activity

Madelon Q. Wentink[a], Tilman M. Hackeng[b], Sebastien P. Tabruyn[a,1], Wouter C. Puijk[c], Klaus Schwamborn[c,2], Daniele Altschuh[d,3], Rob H. Meloen[c], Teun Schuurman[e], Arjan W. Griffioen[a,4,5], and Peter Timmerman[c,f,4,5]

[a]Angiogenesis Laboratory, Department of Medical Oncology, Vrije Universiteit Medical Center, 1081 HZ Amsterdam, The Netherlands; [b]Department of Biochemistry, Maastricht University Medical Center, 6229 HX Maastricht, The Netherlands; [c]Pepscan Therapeutics B.V., 8243 RC Lelystad, The Netherlands; [d]Equipe labellisée Ligue 2015, UMR 7242, Université de Strasbourg, CNRS, École Supérieure de Biotechnologie de Strasbourg, 67412 Illkirch, France; [e]Animal Sciences Group, Wageningen University and Research, 6708 WD Wageningen, Lelystad, The Netherlands; and [f]Van't Hoff Institute of Molecular Sciences, University of Amsterdam, 1098 HX Amsterdam, The Netherlands

Edited by David A. Cheresh, University of California San Diego, La Jolla, CA, and accepted by Editorial Board Member Rakesh K. Jain September 19, 2016 (received for review June 24, 2016)

Therapeutic targeting of the VEGF signaling axis by the VEGF-neutralizing monoclonal antibody bevacizumab has clearly demonstrated clinical benefit in cancer patients. To improve this strategy using a polyclonal approach, we developed a vaccine targeting VEGF using 3D-structured peptides that mimic the bevacizumab binding site. An in-depth study on peptide optimization showed that the antigen's 3D structure is essential to achieve neutralizing antibody responses. Peptide 1 adopts a clear secondary, native-like structure, including the typical cysteine-knot fold, as evidenced by CD spectroscopy. Binding and competition studies with bevacizumab in ELISA and surface plasmon resonance analysis revealed that peptide 1 represents the complete bevacizumab binding site, including the hairpin loop (β5–turn–β6) and the structure-supporting β2–α2–β3 loop. Vaccination with peptide 1 elicited high titers of cross-reactive antibodies to VEGF, with potent neutralizing activity. Moreover, vaccination-induced antisera displayed strong angiostatic and tumor-growth-inhibiting properties in a preclinical mouse model for colorectal carcinoma, whereas antibodies raised with peptides exclusively encompassing the β5–turn–β6 loop (peptides 15 and 20) did not. Immunization with peptide 1 or 7 (murine analog of 1) in combination with the potent adjuvant raffinose fatty acid sulfate ester (RFASE) showed significant inhibition of tumor growth in the B16F10 murine melanoma model. Based on these data, we conclude that this vaccination technology, which is currently being investigated in a phase I clinical trial (NCT02237638), can potentially outperform currently applied anti-VEGF therapeutics.

VEGF | angiogenesis | immunization | protein mimicry | peptide vaccines

Vascular endothelial growth factor (VEGF) is frequently investigated as a target in anticancer therapy (1–3). VEGF contains a "cysteine-knot" motif, which is crucial for proper folding and biological activity (4), and VEGF receptor 2 (VEGFR2) is the predominant mediator of its proangiogenic effects (3).

In combination with chemotherapy, treatment with the monoclonal anti-VEGF antibody bevacizumab has shown clinical benefit in a number of different tumor types (5–7). There is growing evidence that long-term treatment with bevacizumab can be beneficial (8, 9), even beyond disease progression while on bevacizumab-containing therapy. Generating anti-VEGF antibodies through active immunization could offer important advantages. Application would (*i*) only need few intramuscular injections, (*ii*) induce antibodies with superior VEGF-neutralizing ability compared with bevacizumab, (*iii*) provide durable VEGF suppression and reduce the number of hospital visits, and (*iv*) be more cost-effective, overcoming the socioeconomic problems of prohibitively high treatment costs (10).

Over the past decades, the interplay of the immune system and angiogenesis has been further clarified (11). Angiogenic growth factors contribute to immune suppression by down-regulation of endothelial adhesion molecules (12–14), inhibition of dendritic cell maturation (15), and attraction and proliferation of immunosuppressive cells (16, 17). Conversely, antiangiogenic drugs can help reverse the immunosuppressive state in cancer patients (14, 18, 19). Therefore, an angiostatic vaccination approach against VEGF can potentially inhibit tumor growth via multiple mechanisms (20).

Preclinical evidence for the antitumor activity of VEGF-vaccination strategies has been provided (21, 22), showing the safety of this approach. Recently, phase I clinical data with a VEGF vaccine (23) in patients with advanced cancer was reported. This treatment appeared to be safe, and common anti-VEGF–related adverse events were absent.

However, vaccination with intact VEGF has major drawbacks, such as unwanted biological activity and weak immunogenicity,

Significance

VEGF is the pivotal growth factor for angiogenesis, and its inhibition by passive immunotherapy results in improved survival in patients with several types of cancer. We believe that the clinical benefit could be increased by inducing a humoral immune response against VEGF through active immunization with VEGF-based peptides. In this study, we describe that correct peptide design is vital for success. We show that only 3D-structured peptides perfectly mimicking the crucial β5–turn–β6 loop of endogenous VEGF are able to induce neutralizing antibodies. We developed a vaccine with potent in vitro and in vivo VEGF-neutralizing activities, as shown in passive and active immunization tumor models. The VEGF vaccination strategy has the potential to outperform current clinical anti-VEGF treatment strategies.

Author contributions: T.M.H., R.H.M., A.W.G., and P.T. designed research; M.Q.W., T.M.H., S.P.T., W.C.P., K.S., D.A., T.S., and P.T. performed research; M.Q.W., T.M.H., S.P.T., W.C.P., K.S., D.A., R.H.M., T.S., A.W.G., and P.T. analyzed data; and M.Q.W., A.W.G., and P.T. wrote the paper.

Conflict of interest statement: The presented vaccination technology was patent-protected by the inventors T.M.H., A.W.G., and P.T. The patent is licensed by Immunovo BV, Den Bosch, The Netherlands.

This article is a PNAS Direct Submission. D.A.C. is a Guest Editor invited by the Editorial Board.

[1]Present address: TransCure bioServices, FR-74160 Archamps Technopôle, France.

[2]Present address: Valneva SE 6, Rue Alain Bombard, 44800 Saint-Herblain, Nantes, France.

[3]Present address: Department of Integrative Biology, Institute of Genetics and Molecular and Cellular Biology, CNRS UMR 7104, INSERM U 964, Université de Strasbourg, Illkirch, France.

[4]A.W.G. and P.T. contributed equally to this work.

[5]To whom correspondence may be addressed. Email: p.timmerman@pepscan.com or aw.griffioen@vumc.nl.

This article contains supporting information online at www.pnas.org/lookup/suppl/doi:10.1073/pnas.1610258113/-/DCSupplemental.

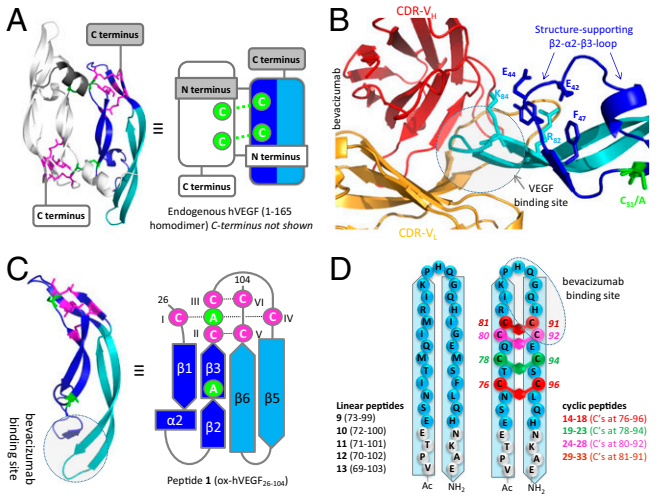

Fig. 1. Graphical representation of all constructed VEGF mimics. (*A*) Ball-and-stick and schematic representation of $hVEGF_{165}$. (*B*) Ball-and-stick representation of the binding of bevacizumab to VEGF. The picture illustrates that the antibody-binding β5–turn–β6 loop (in light blue) is structurally supported by the β2–α2–β3 loop (in dark blue). (*C*) Ball-and-stick and schematic representation of folded peptide **1** (including the intact cysteine-knot fold in blue). Cysteines (and mutated alanines) that form the two disulfide bonds covalently linking the individual subunits in the homodimer are indicated in green. In its folded state, this peptide provides the smallest possible mimic of the bevacizumab-binding site on $hVEGF_{165}$. (*D*) Schematic representation of linear and xylene-bridged peptides 9–33.

requiring chemical inactivation and/or protein conjugation (21). Using modified antigens, however, may give rise to antibodies lacking neutralizing properties. Alternative strategies using human VEGF (hVEGF)-derived peptides (24) appeared moderately successful (25, 26). We show that induction of neutralizing antibodies with tumor-growth-inhibiting power was only successful for a 3D-structured 79-mer peptide (**1**; ox-$hVEGF_{26–104}$) with a fully intact cysteine-knot fold that covers the complete discontinuous binding site of bevacizumab. Crucial to its activity is that peptide **1** adopts a native-like VEGF structure in solution and that it binds to bevacizumab with near equal affinity as $hVEGF_{165}$. Eradication of tumor growth using peptide **1** was demonstrated in two different tumor models.

Results

Design and Synthesis of VEGF Peptide Mimics. Because virtually all antibody-binding sites are discontinuous in nature (27), a total of 33 peptide mimics of VEGF with varying levels of structural complexity (linear, conformational, and discontinuous) were designed, synthesized, and tested for bevacizumab binding and the ability to generate potent antisera with cross-reactivity to and neutralizing ability for $hVEGF_{165}$ (Fig. 1). The 79-mer peptide **1** [molecular mass (MM) = 9.1 kDa, ∼25% of $hVEGF_{165}$], starting at C_I and ending at C_{VI} of the cysteine-knot fold (*SI Appendix*, Table S1), mimics the bevacizumab binding site in its most native form (Fig. 1*A*). It contains both the β5–turn–β6 hairpin loop, as well as the β2–α2–β3 loop, which stabilizes and positions the β5–turn–β6 loop for bevacizumab binding (28, 29) (Fig. 1*B*). Cysteines C_{51} and C_{60}, which covalently link the subunits in $hVEGF_{165}$ via two disulfide bonds (30), were replaced by alanines to block homodimerization and thus prevent agonistic VEGF-like activity (Fig. 1 *B* and *C*). In addition, the rat (**6**) and mouse (**7**) variants were synthesized (*SI Appendix*, Table S1).

Folding of peptides **1**, **6**, and **7** produced the intact cysteine-knot fold in <2 h (*SI Appendix*, Fig. S1*A*), which is considerably shorter than folding of native $hVEGF_{165}$, which takes ∼5 d (31). Both MALDI-TOF MS (*SI Appendix*, Fig. S1*B*) and electrospray ionization-MS (*SI Appendix*, Fig. S2 and Table S2) confirmed formation of the cysteine-knot fold as judged from the 6-Da reduction in MM for folded peptide **1** (MM_{exp} = 9,060.6) compared with unfolded peptide **1** (MM_{exp} = 9,066.6; *SI Appendix*, Fig. S1*B*).

To evaluate the relevance of structural folding for bevacizumab binding and the ability to generate neutralizing anti-VEGF antibodies, we synthesized three SS-deletion variants of peptide **1**, each lacking one of three SS bonds in the native cysteine-knot fold (*SI Appendix*, Table S1). In addition, a variant lacking all three cysteine-knot SS bonds (peptide **5**) was prepared via reaction of reduced peptide **1** with excess of iodoacetamide (*SI Appendix*, Table S1).

The bevacizumab epitope is reported to be linear or conformational and located at the top of the β5–turn–β6 loop (amino acids 85–92) (29). Accordingly, we included 5 linear (**9–13**) peptides and 20 different side-chain cyclized peptides (**14–33**) covering this region (Fig. 1*D* and *SI Appendix*, Table S3). For each cyclic peptide, an adjacent pair of native amino acids was replaced by a pair of cysteines that were subsequently connected by using a *meta*-xylene bridge (32, 33) (*SI Appendix*, Table S3).

In Vitro Activities of VEGF Mimics 1–33. Binding of folded peptide **1** to bevacizumab was studied in detail. Bevacizumab binds surface-immobilized **1** even at low concentrations [negative logarithm of EC_{50} (pEC_{50}) = 4.5; Fig. 2*A*] and with comparable intensity to $hVEGF_{165}$ (pEC_{50} = 4.8). Competition studies showed that peptide **1** and $hVEGF_{165}$ inhibit the binding of bevacizumab to surface-immobilized $hVEGF_{165}$ with almost similar strength (IC_{50} = 19.4 nM for peptide **1** and 6.2 nM for $hVEGF_{165}$; Fig. 2*B*). Bevacizumab binding was fully specific for the human VEGF sequence (i.e., peptide **1**), because binding was observed with neither the rat (**6**) nor the mouse (**7**) variants (Fig. 2*A* and *SI Appendix*, Fig. S3*B*). The 1:1-affinity constant (K_D) for the binding of bevacizumab to peptide **1** was 1.01 ± 1.09 nM using BIACORE affinity

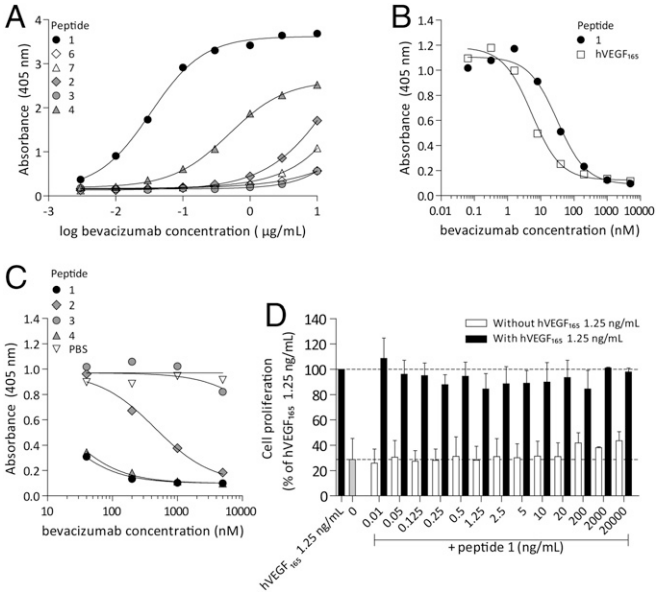

Fig. 2. $hVEGF_{165}$ and peptide **1** have similar binding properties whereas the activity of SS-deletion variants is reduced. (*A*) Peptide **1** strongly binds bevacizumab, and peptide **4** has intermediate bevacizumab binding capacities, whereas peptides **2**, **3**, **6**, and **7** have virtually no binding capacities with bevacizumab. (*B*) $hVEGF_{165}$ and peptide **1** are equally well able to inhibit the binding of bevacizumab to plate-bound $hVEGF_{165}$ in a competition ELISA. (*C*) Peptides **1** and **4** are able to inhibit the binding of bevacizumab to $hVEGF_{165}$, whereas peptides **2** and **3** are not able to inhibit the binding of bevacizumab to $hVEGF_{165}$ in a competition ELISA. (*D*) Peptide **1** does not stimulate cell proliferation of VEGF dependent Ba/F3–VEGFR2 cells, nor does it affect the Ba/F3–VEGFR2 cell proliferation-promoting effects of $hVEGF_{165}$.

measurements (*SI Appendix*, Fig. S4), which compares well with the reported K_D value for bevacizumab and $hVEGF_{165}$ of 2.2 nM (34).

To clarify the importance of an intact cysteine-knot fold for bevacizumab binding, and in particular the contribution of each individual SS-bond, we also studied the binding to the three SS-deletion variants (**2–4**) as well as to the fully unfolded peptide **5** and (unstructured) peptides **9–33**. Peptide **4** bound with a ∼16-fold lower affinity to bevacizumab (pEC_{50} = 3.3; Fig. 2*A* and *SI Appendix*, Fig. S3*A*), but was virtually as active as peptide **1** at inhibiting the binding of bevacizumab to $hVEGF_{165}$ (IC_{50} = 16 nM for peptide **4**) (Fig. 2*C*), whereas for variants **2** and **3**, binding was almost completely lost (pEC_{50} = 2.0 and <2 and IC_{50} = 432 nM and >10 μM for **2** and **3** respectively; Fig. 2 *B* and *C* and *SI Appendix*, Fig. S3*A*). Neither the linear peptides **9–13** nor the unstructured peptide **5** showed measurable binding up to 10 μg/mL (*SI Appendix*, Fig. S3*A*). However, the xylene-bridged peptides **14–17** (C_{76}–C_{96}) and **19–22** (C_{78}–C_{94}) also showed prominent binding to bevacizumab (pEC_{50} up to 3.3), thus confirming the conformational nature of the binding site.

We also studied the ability of peptide **1** to either agonize or antagonize VEGF-dependent cell proliferation of Ba/F3 cells, engineered to express VEGFR2. No detectable increase in cell viability was observed in Ba/F3–VEGFR2 cells when incubated with peptide **1** (Fig. 2*D*). Similarly, peptide **1** also did not markedly reduce cell proliferation when cultured with 1.25 ng/mL $hVEGF_{165}$ (Fig. 2*D*). These data show that peptide **1** is fully devoid of agonistic or antagonistic activity toward $hVEGF_{165}$ or VEGFR2.

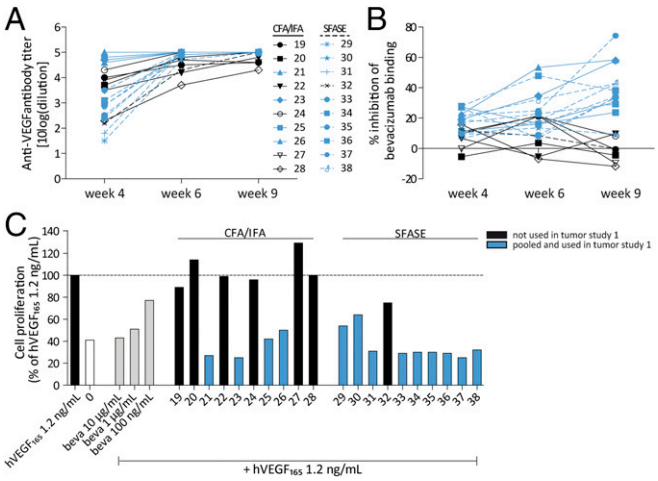

Fig. 3. Immunization with peptide **1** induces a strong anti-VEGF neutralizing antibody response. (*A*) Immunization of Wistar rats with peptide **1** adjuvated with CFA/IFA or SFASE induces high titer antibodies cross-reactive with $hVEGF_{165}$. (*B*) Immunization-induced antibodies inhibit the binding of bevacizumab to $hVEGF_{165}$ in a competition ELISA. Antisera were used in 1:400 dilutions. (*C*) Antisera obtained 9 wk after the final immunization (in 1:100 dilution) coincubated with 1.2 ng/mL $hVEGF_{165}$ inhibit the proliferation of Ba/F3–VEGFR2 cells. Antisera used in 1:200 dilutions gave similar results.

Immunization Studies with VEGF Mimics 1–33. The immunogenicity of peptide **1** was studied in different species. Adjuvants used included the conventional complete/incomplete Freund's adjuvant (CFA/IFA) and the novel adjuvant sucrose fatty acid sulfate ester (SFASE) (*SI Appendix*, section 3.2). In Wistar rats immunized with peptide **1**, we detected high antibody titers against peptide **1** 9 wk after primer immunization (antibody titer of 5.3; *SI Appendix*, Table S6), as well as against $hVEGF_{165}$ (antibody titers of 5.2 to >5.4; Fig. 3*A* and *SI Appendix*, Tables S5 and S6). Immunization studies in BALB/c mice showed similar results (*SI Appendix*, Table S5). Moreover, antisera induced in Wistar rats were found to block the binding of bevacizumab to surface-immobilized $hVEGF_{165}$ in a competition ELISA (Fig. 3*B*) and showed near complete inhibition (>95% compared with hVEGF 1.2 ng/mL) of VEGF-dependent cell proliferation in the Ba/F3–VEGFR2 cell-based bioassay (Fig. 3*C* and *SI Appendix*, Fig. S8). Although peptide **1** adjuvated with CFA/IFA or SFASE induced similar antibody titers against $hVEGF_{165}$, SFASE antisera seemed to outperform CFA/IFA antisera in VEGF-neutralizing abilities, given the superior results in the competition ELISA as well as the Ba/F3–VEGFR2 cell proliferation assay (Fig. 3 *B* and *C*).

Immunization with linear and cyclized peptides covering the β5–turn–β6 loop (peptides **9–33**) induced high-titer antibodies cross-reactive with $hVEGF_{165}$ as well (mean antibody titer ± SD: 4.6 ± 0.7; *SI Appendix*, Fig. S7). However, antisera induced by immunization with peptides **15** and **20** in a larger experiment were not able to neutralize the biological activity of VEGF in the Ba/F3–VEGFR2 cell proliferation assay (mean cell proliferation compared with $hVEGF_{165}$ 1.25 ng/mL using nonpurified sera ± SD; 90.1% ± 13.9%; *SI Appendix*, Table S8). In addition, immunization with SS-deletion variant peptides **2–4** also induced high anti-VEGF antibody titers (mean antibody titer ± SD; 4.6 ± 0.2; *SI Appendix*, Table S7), whereas VEGF-driven proliferation of Ba/F3–VEGFR2 cells remained unaffected when treated with these sera (mean cell proliferation compared with $hVEGF_{165}$ 1.25 ng/mL ± SD; 104.2% ± 14.3%; *SI Appendix*, Table S7), indicating that antibodies induced with these deletion variants were also devoid of $hVEGF_{165}$-neutralizing properties.

Antiangiogenic and Antitumor Activity by Vaccination Against VEGF. ***Passive Immunization with VEGF-Based Peptides in LS174T Human Colon Cancer Xenografts.*** The most neutralizing sera in Wistar rats (blue bars in Fig. 3*C*) were pooled, and the IgG fraction was purified and used to treat LS174T-bearing immunodeficient mice. A very clear and marked inhibition of tumor growth was observed after treatment with antipeptide **1** (group 3) or bevacizumab (group 2), compared with PBS-treated mice (group 1; $P < 0.001$; Fig. 4 *B* and *C*). Both treatments were well tolerated, as evaluated by survival of the animals, overall behavior, and body weight (*SI Appendix*, Fig. S9). As shown in Fig. 4*D*, the microvessel density in antipeptide **1**- and bevacizumab-treated tumors was markedly reduced ($P < 0.001$), suggesting that the antitumor effects are due to angiogenesis inhibition.

In parallel, the effects of antisera elicited with β5–turn–β6 loop peptide (**15** and **20**) immunization were studied in the same tumor model. LS174 T tumor growth again showed to be very sensitive to anti-VEGF treatment, given the clear antitumor effects of bevacizumab treatment ($P < 0.001$; *SI Appendix*, Fig. S10). In contrast, tumor growth of antipeptides **15** and **20** antisera-treated mice was unaffected compared with PBS-treated mice (*SI Appendix*, Fig. S10), showing that these antisera, which were unable to neutralize VEGF in vitro, indeed do not exhibit tumor growth inhibition properties.

Active Immunization Inhibits Tumor Growth in the B16F10 Murine Melanoma Model. In a final experiment, we investigated whether vaccination in a syngeneic tumor model with peptides **1** (group 5), **7** (mouse variant of **1**; group 4), and **8** (unstructured variant of **7**; group 3) in mice could inhibit tumor growth. For this study, raffinose fatty acid sulfate ester (RFASE) adjuvant was used instead of SFASE adjuvant because of its more optimal properties for clinical development (*SI Appendix*, section 3.2). Mice treated with PBS (group 1) or RFASE alone (group 2) served as controls. C57BL/6 mice received four intramuscular injections with these peptides adjuvated with RFASE with 2-wk intervals (Fig. 5*A* and *SI Appendix*, section 3.5). One mouse in group 5 died shortly after the third immunization. Moreover, 50% of the mice of groups 4 and 5 displayed hunched posture, lethargy, and piloerection immediately after the third immunization. Moreover, these symptoms were observed in all animals of groups 3–5 right after the fourth immunization and also increased in severity. In total, 11 mice (6 in group 5, 4 in group 4, and 1 in group 3) died after the final booster. All remaining mice recovered within 1 h after immunization. Body weights were unaffected in all mice throughout

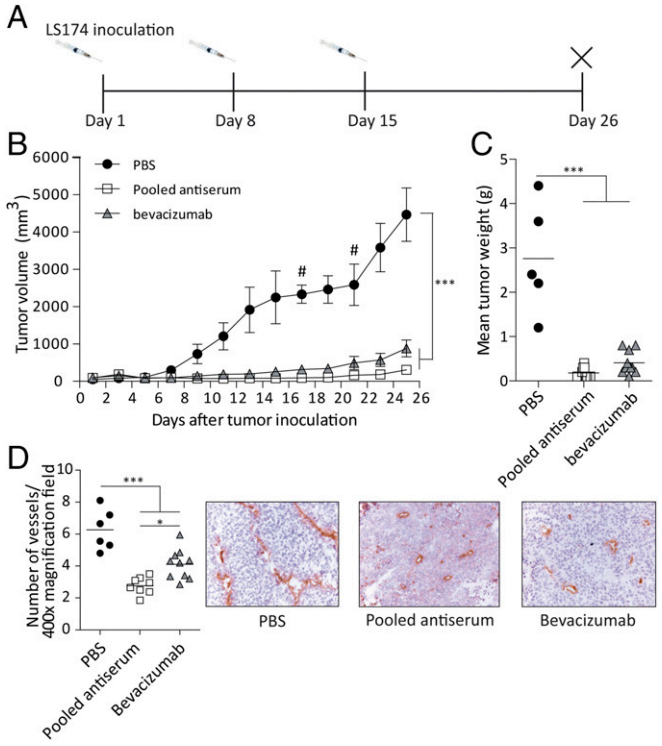

Fig. 4. Pooled rat peptide **1** antisera have potent tumor-inhibiting and anti-angiogenic properties. (*A*) Design of the study. (*B* and *C*) Treatment with pooled antiserum as well as bevacizumab inhibited the growth of LS174T human colon carcinoma compared with PBS-treated tumors, as quantified by tumor volume and tumor weight. Data are expressed as mean ± SEM ($n = 9$ or 10 per group). (*D*) Intratumoral MVD in pooled antiserum and bevacizumab-treated tumors was reduced compared with PBS-treated tumors. Data are expressed as mean ± SEM ($n = 9$ or 10 per group). # is animals out of study. $^*P < 0.05$; $^{***}P < 0.001$.

the study (*SI Appendix*, Fig. S11). Furthermore, other toxicities were not observed in any of the immunized mice.

Ten days after the fourth immunization, mice were inoculated with 10^5 B16F10 murine melanoma cells (Fig. 5*A*). Cross-reactive antibodies against $mVEGF_{164}$ were found in all mice of groups 3–5 (Fig. 5*B*). Counterintuitively, serum mouse VEGF concentrations were markedly increased in mice of groups 4 and 5 (Fig. 5*C*). On day 21, tumor growth of mice immunized with peptides **1** or **7** (groups 4 and 5), but not those immunized with unstructured peptide **8**, was significantly inhibited, compared with PBS-treated mice ($P < 0.001$; Fig. 5*D*).

Discussion

Treating advanced cancer using antiangiogenesis therapy (bevacizumab, VEGF-trap) combined with chemotherapy is known to prolong survival in several tumor types (5–7). However, the clinical benefit is fairly modest, urging researchers to discover improved treatment strategies. (Pre)clinical studies have shown that continuous and prolonged exposure as opposed to discontinuous VEGF suppression provides maximum benefit (8, 35). The ideal way to meet this objective is by targeting vascular epitopes via active immunization (10).

In this work, we describe data from both immunization and tumor-suppression studies using the 79-mer peptide **1** (ox-$hVEGF_{26–104}$) that reconstitutes the conformational and discontinuous binding site of bevacizumab on $hVEGF_{165}$. We provide evidence that enforcing a native-like, secondary structure in **1** is the key to success for inducing neutralizing anti-hVEGF antibodies with tumor-inhibiting power. According to X-ray data, the β2/α2-loop residues $E_{42}/E_{44}/Y_{45}/F_{47}$ in **1** have a structure-stabilizing interaction with the β5–turn–β6 loop residues R_{82}/K_{84} (Fig. 1*C*), which correctly positions this loop for bevacizumab binding (29). We anticipate that the presence of this structure-stabilizing loop is critical for generating a potent and neutralizing antibody response.

Peptide **1** is strongly immunogenic and does not require conjugation to a carrier protein, despite the fact that it is derived from an endogenous protein. Truncation of native $hVEGF_{165}$ to 79 amino acids ($hVEGF_{26–104}$), as well as substitution of C_{51} and C_{60} for alanines, likely gives rise to neo-epitopes that increase its immunogenicity (36). Immunizations with peptide **1** raised potent anti-VEGF antisera with strong neutralizing activity in VEGF-dependent Ba/F3–VEGFR2 bioassay (Fig. 3*C* and *SI Appendix*, Fig. S8) and the ability to inhibit bevacizumab-binding to $hVEGF_{165}$ in ELISA (Fig. 3*B*). Peptide **1** is monomeric in nature, unlike the homodimeric $VEGF_{165}$ protein, and therefore neither agonizes nor antagonizes VEGF-dependent proliferation in Ba/F3–VEGFR2 cells (Fig. 2*D*). This feature makes peptide **1** the perfect immunogen for development of an anti-VEGF vaccine. Peptide **1** can be administered safely in vivo without the risk of interfering with endogenous VEGF signaling. Interestingly, antisera raised against peptide **1** showed significantly weaker binding to unstructured peptides **2**, **3**, and **5** in ELISA (*SI Appendix*, Table S7), indicating that anti-peptide **1** antibodies mainly recognize conformational and/or discontinuous epitopes.

The type of adjuvant used also appears to influence the neutralizing capacity of the resulting antisera to an appreciable extent. Immunization with the "oil-in-water emulsion" SFASE adjuvant induced neutralizing antisera in 9 of 10 animals (animals 29–38; Fig. 3*C*), whereas appreciable VEGF-neutralizing ability was only observed in 4 of 10 antisera using the "water-in-oil emulsion" adjuvant CFA/IFA (animals 19–28; Fig. 3*C*). This marked difference might be due to the oily component of CFA/IFA causing partial or complete unfolding of peptide **1**, thus

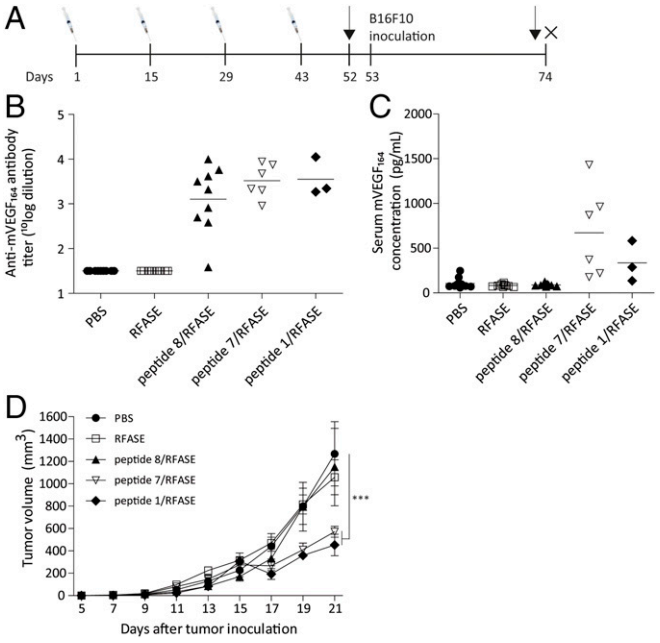

Fig. 5. Active immunizations with peptides **1** and **7** inhibit the growth of B16F10 melanoma. (*A*) Design of the study. (*B*) Immunization with peptide **8**/RFASE, peptide **7**/RFASE, and peptide **1**/RFASE induces cross-reactive antibodies against $hVEGF_{165}$. (*C*) Immunization with peptide **7**/RFASE and peptide **1**/RFASE induces an increase in serum mouse VEGF concentration. (*D*) Immunization with peptide **7**/RFASE and peptide **1**/RFASE significantly inhibits the growth of B16F10 melanoma, whereas peptide **8**/RFASE immunized mice developed tumors not statistically significantly smaller than PBS-treated mice. Data are shown as mean ± SEM ($n = 3–10$ per group). $^{***}P < 0.001$.

generating antibodies that no longer recognize or neutralize endogenous VEGF (see below).

Passive immunization of Swiss nu/nu mice with a mixture of the 13 most potent antisera raised against peptide **1** completely inhibited the growth of LS174T colon carcinoma, to the same extent as bevacizumab treatment (Fig. 4 *B–D*). Additionally, active immunization with the 3D-folded peptides **1** (human variant) and **7** (mouse variant) significantly inhibited the growth of B16F10 melanoma in C57BL/6 mice (Fig. 5*D*), whereas the analogous unstructured peptide **8** was totally ineffective. These data emphasize that only correctly folded peptides are able to induce antibodies that neutralize VEGF and thus able to inhibit tumor angiogenesis. Furthermore, this experiment confirms that truncation is sufficient to break immune self-tolerance, because immunization with the mouse homolog peptide **7** induced antibodies with similar antitumor properties as peptide **1**. Much to our surprise, an increase instead of a significant decrease in serum mouse VEGF (mVEGF) levels was observed for peptide **1**- and **7**-immunized mice. This result is most likely due to reduced clearance of the antibody·mVEGF immune complexes formed, which are known to clear slower than free mVEGF (37). Again, the fact that serum mVEGF levels were unaffected in peptide **8**-treated mice suggests that the antibodies induced in this group are unable to recognize endogenous mVEGF. Because we did observe a significant reduction in tumor growth for peptide **1**- and **7**-immunized mice, it appears that these immune complexes do not interfere with tumor growth inhibition and apparently have no biological function. A positive correlation between mVEGF-levels and anti-mVEGF antibody titers was only observed for peptide **7**-immunized mice (*SI Appendix*, Fig. S12*B*), whereas this was not the case in peptides **1** and **8** (*SI Appendix*, Fig. S12 *A* and *C*). Even though our conclusions for peptide **1** might be somewhat premature as a result of the low number of animals in group 5, the lack of correlation for peptide **8**-immunized mice clearly stresses the inability of peptide-**8**-induced antibodies to bind mVEGF.

Even though repeated immunization with peptide **1**/RFASE did not lead to overt toxicity in Wistar rats, several C57BL/6 mice died shortly after the third or fourth booster immunizations. We hypothesize that this event was caused by an antigen-specific IgE- or IgG-mediated anaphylactic response, which only occurred in mice due to the relatively high doses of antigen given (~10 μg per g for mice vs. <1 μg per g of body weight for all other animals). Interestingly, mice immunized with RFASE adjuvant alone did not develop similar symptoms, excluding the possibility that the adjuvant was responsible for the observed adverse effects.

We did not specifically address the duration of the immune response, but various reports evidently show that immune responses raised against endogenous antigens are fully reversible (38–42). Long-term data with a peptide-based GnRH-targeting cancer vaccine for testosterone deprivation, also developed by us (43), showed that testosterone levels reappeared ~30 wk later (43), showing that anti-GnRH immunity is indeed reversible. We therefore anticipate that duration of the peptide **1**/RFASE immune response will be comparable, which would require regular revaccination to maintain high antibody titers. Importantly, it is highly unlikely that endogenous VEGF will serve as booster after immunization with peptide **1**/RFASE, because (*i*) exposure to endogenous VEGF occurs in the absence of RFASE adjuvant, and (*ii*) it is improbable that CD4 T-cell help for endogenous VEGF is generated as activation of CD4 T cells after immunization was only possible through truncation and modification of endogenous VEGF into the immunogen peptide **1**.

It is not likely that our vaccination strategy results in cellular immunity. First, the vaccine is administered through intramuscular injections, a route more likely to skew toward humoral immunity. Second, long peptides as immunogens are less prone to induce cellular immunity compared with DNA vaccines; exogenous peptides require cross-presentation to be able to be presented by MHC I to induce cellular immunity, whereas they can be directly presented in the context of MHC II to CD4 helper T cells.

Several studies have claimed success with vaccines based on peptides derived from either $hVEGF_{165}$ or VEGFR2 (21, 24, 26). Most of these involved the use of linear or unstructured peptides. However, all our efforts to obtain antisera with notable neutralizing capacity in the Ba/F3–VEGFR2 cell assay (*SI Appendix*, Table S8) and/or tumor-inhibiting power (*SI Appendix*, Table S10) using constrained β5–turn–β6 loop peptides **15** and **20** failed. This finding clearly disqualifies the hypothesis that the binding site of bevacizumab is linear or conformational (29) and supports our view that a structurally complex peptide like **1** is indeed required to reconstitute the bevacizumab binding site entirely. Immunization with peptides **2–5**, lacking either one (**2–4**) or all (**5**) SS bonds of the structure-supporting cysteine-knot fold in peptide **1**, only raised antisera completely devoid of neutralizing activity for hVEGF (*SI Appendix*, Table S7).

There is a lack of effective methods classifying good or poor peptide immunogens for $hVEGF_{165}$. We learnt that measuring $hVEGF_{165}$ cross-reactivity of peptide antisera in ELISA is clearly not a good indicator, because antisera elicited by misfolded or unfolded peptides (e.g., **5** and **14–18**) also harbored antibodies binding extremely strongly to $hVEGF_{165}$ in ELISA (titers 5.4 or higher; *SI Appendix*, Table S7 and Fig. S7). This result is likely due to (partial) denaturation of $hVEGF_{165}$ upon surface immobilization to the ELISA plate. Instead, we discovered that measuring (*i*) the binding of bevacizumab to the peptides or (*ii*) the ability of the peptides to inhibit binding of bevacizumab to $hVEGF_{165}$ provides a much better predictor for success. As expected, peptide **1** was the minimal peptide to show high-affinity binding to bevacizumab with SPR and in ELISA and showed strong competition of bevacizumab-binding to surface-immobilized $hVEGF_{165}$, whereas unstructured peptides like **2**, **3**, **5**, and **14–33** showed much weaker or no binding to bevacizumab in ELISA (*SI Appendix*, Fig. S3 *A* and *C*), nor did they inhibit binding of bevacizumab to $hVEGF_{165}$.

Materials and Methods

Cell Lines and Reagents. The Ba/F3–VEGFR2 cells were a kind gift from K. Alitalo (Institute of Biomedicine, Biomedicum Helsinki, Helsinki, Finland) and were licensed by the Ludwig Institute for Cancer Research. Ba/F3 cells are transfected with a receptor consisting of the extracellular domain of VEGFR2 and the transmembrane and cytoplasmic domain of mouse erythropoietin receptor (44, 45), making them dependent on VEGF or mIL3 for proliferation and survival. Ba/F3–VEGFR2 cells were maintained as suspension cultures in complete medium [DMEM (Lonza) supplemented with 10% (vol/vol) heat-inactivated (HI) FBS (BioWest SAS), Pen-Strep (Lonza), L-glutamin (2 mM; Scharlab S.L), mIL3 (4 ng/mL; R&D Systems), zeocin (500 μg/mL; Invitrogen)] in an atmosphere of 5% (vol/vol) CO_2 at 37 °C. The murine melanoma cell line B16F10 and the human colon cancer cell line LS174T were purchased from the American Type Culture Collection and were cultured in DMEM supplemented with 10% (vol/vol) HI FBS, Pen-Strep, and L-glutamin.

Ba/F3–VEGFR2 Bioassay. Complete medium (see above) containing hVEGF (1.25 ng/mL; R&D Systems) was preincubated with serum containing anti-VEGF antibodies and plated in a 96-well plate for 1 h at 37 °C. Ba/F3–VEGFR2 cells were added at a concentration of 2×10^5 cells per mL and incubated for 72 h. Cell proliferation was quantified with WST-1 (Roche Applied Science). Optical density was measured with a TecanSpectrafluor plate reader at a wavelength of 450 nm and a reference wavelength of 600 nm. The proliferation of cells on serum from vaccinated animals was calculated as percentage of cell proliferation when cultured with hVEGF alone.

Vaccine Preparation. The synthesis of all VEGF-derived peptides and BIACORE affinity measurements, as well as a detailed description on vaccine preparation, are described in *SI Appendix*, section 3.2. Briefly, the peptides were mixed with the adjuvants RFASE, SFASE (46, 47), or CFA/IFA.

Immunization Studies. Animal experiments were approved by the local ethical review committee (Wageningen University and Research). Detailed procedures for these studies are described in *SI Appendix*, section 3.5. In summary, studies 1 and 2 were passive immunization studies in which LS174T colon cancer-bearing immunodeficient Swiss nu/nu mice were treated with antisera recognizing $hVEGF_{165}$ that were generated in Wistar rats. For study 1,

rats were immunized with the 3D-structured peptide **1**, whereas for study 2, rats were immunized with either the linear or cyclic peptides **9–13** derived of the β5–turn–β6 region of $hVEGF_{165}$ (amino acids 69–103). Refer to Fig. 4*A* for the study design of both experiments. In study 3, C57BL/6 mice were prophylactically immunized with 175 μL of peptide **8**/RFASE (group 3), peptide **7**/RFASE (group 4), or peptide **1**/RFASE (group 5). Control mice received either RFASE (group 2) or PBS (group 1) alone. Ten days after the last immunization, the mice were challenged with 5×10^4 B16F10 murine melanoma cells. The tumors were allowed to grow for 21 d (Fig. 5*A*).

Histological Analysis in Xenograft Tumors. CD31 was detected by immunohistochemical staining on solid LS174 T tumors. Five-micrometer sections were stained for CD31 with hematoxylin as counterstain. Tissues were fixed in acetone for 15 min at −20 °C. Endogenous peroxidase was blocked with 3% (mass/mass) H_2O_2, and aspecific binding was prohibited by treatment with 5% (mass/mass) BSA. Primary and secondary antibodies used were rat–anti-mouse CD31 (BD Biosciences Pharmingen; 1:100 dilution) and donkey–anti-rat IgG (Jackson; 1:300 dilution). Hereafter, the tissues were incubated with streptavidin–HRP (Dako; 1:300 dilution). HRP was detected by the addition of 3,3′-diaminobenzidine (Envision kit; Dako; 1:50 dilution). Intratumoral microvessel density (MVD) was calculated by taking the mean of vessel counts in 10 random fields at 400× magnification.

Statistical Analysis. The repeated-measured two-way ANOVA with Bonferroni posttest was used for repeated measurements at different time points (Figs. 4*B* and 5*D*). For tumor weight comparisons (Fig. 4*C*) and MVD in tumor sections (Fig. 4*D*), one-way ANOVA with Dunnett's posttest was used. $P < 0.05$ were considered significant. All analyses were performed by using GraphPad Prism (Version 5.00 for Windows; GraphPad Software).

ACKNOWLEDGMENTS. We thank Ronald Boshuizen, Johan Turkstra, Jan van der Meulen, and Franz Jozef van der Staay for assistance with the preclinical studies; Dr. Kari Alitalo (Institute of Biomedicine, Biomedicum Helsinki) for providing the Ba/F3–VEGFR2 cells; and Dennis Suylen for assistance with peptide synthesis. This work was supported by the IS program of Senter-Novem (Grant IS052039) and Immunovo BV.

1. Folkman J (1971) Tumor angiogenesis: Therapeutic implications. *N Engl J Med* 285(21):1182–1186.
2. Griffioen AW, Molema G (2000) Angiogenesis: Potentials for pharmacologic intervention in the treatment of cancer, cardiovascular diseases, and chronic inflammation. *Pharmacol Rev* 52(2):237–268.
3. Ferrara N, Gerber HP, LeCouter J (2003) The biology of VEGF and its receptors. *Nat Med* 9(6):669–676.
4. Iyer S, Acharya KR (2011) Tying the knot: The cystine signature and molecular-recognition processes of the vascular endothelial growth factor family of angiogenic cytokines. *FEBS J* 278(22):4304–4322.
5. Hurwitz H, et al. (2004) Bevacizumab plus irinotecan, fluorouracil, and leucovorin for metastatic colorectal cancer. *N Engl J Med* 350(23):2335–2342.
6. Sandler A, et al. (2006) Paclitaxel-carboplatin alone or with bevacizumab for non-small-cell lung cancer. *N Engl J Med* 355(24):2542–2550.
7. Escudier B, et al. (2010) Phase III trial of bevacizumab plus interferon alfa-2a in patients with metastatic renal cell carcinoma (AVOREN): Final analysis of overall survival. *J Clin Oncol* 28(13):2144–2150.
8. Bennouna J, et al.; ML18147 Study Investigators (2013) Continuation of bevacizumab after first progression in metastatic colorectal cancer (ML18147): A randomised phase 3 trial. *Lancet Oncol* 14(1):29–37.
9. Masi G, et al.; BEBYP Study Investigators (2015) Continuation or reintroduction of bevacizumab beyond progression to first-line therapy in metastatic colorectal cancer: Final results of the randomized BEBYP trial. *Ann Oncol* 26(4):724–730.
10. Wentink MQ, et al. (2015) Vaccination approach to anti-angiogenic treatment of cancer. *Biochim Biophys Acta* 1855(2):155–171.
11. Rivera LB, Bergers G (2015) Intertwined regulation of angiogenesis and immunity by myeloid cells. *Trends Immunol* 36(4):240–249.
12. Griffioen AW, Damen CA, Martinotti S, Blijham GH, Groenewegen G (1996) Endothelial intercellular adhesion molecule-1 expression is suppressed in human malignancies: The role of angiogenic factors. *Cancer Res* 56(5):1111–1117.
13. Griffioen AW, Damen CA, Blijham GH, Groenewegen G (1996) Tumor angiogenesis is accompanied by a decreased inflammatory response of tumor-associated endothelium. *Blood* 88(2):667–673.
14. Dirkx AE, et al. (2003) Tumor angiogenesis modulates leukocyte-vessel wall interactions in vivo by reducing endothelial adhesion molecule expression. *Cancer Res* 63(9):2322–2329.
15. Gabrilovich DI, et al. (1996) Production of vascular endothelial growth factor by human tumors inhibits the functional maturation of dendritic cells. *Nat Med* 2(10):1096–1103.
16. Gabrilovich D, et al. (1998) Vascular endothelial growth factor inhibits the development of dendritic cells and dramatically affects the differentiation of multiple hematopoietic lineages in vivo. *Blood* 92(11):4150–4166.
17. Li B, et al. (2006) Vascular endothelial growth factor blockade reduces intratumoral regulatory T cells and enhances the efficacy of a GM-CSF-secreting cancer immunotherapy. *Clin Cancer Res* 12(22):6808–6816.
18. Dings RP, et al. (2011) Enhancement of T-cell-mediated antitumor response: Angiostatic adjuvant to immunotherapy against cancer. *Clin Cancer Res* 17(10):3134–3145.
19. Dirkx AE, et al. (2006) Anti-angiogenesis therapy can overcome endothelial cell anergy and promote leukocyte-endothelium interactions and infiltration in tumors. *FASEB J* 20(6):621–630.
20. Schoenfeld JD, Dranoff G (2011) Anti-angiogenesis immunotherapy. *Hum Vaccin* 7(9):976–981.
21. Rad FH, et al. (2007) VEGF kinoid vaccine, a therapeutic approach against tumor angiogenesis and metastases. *Proc Natl Acad Sci USA* 104(8):2837–2842.
22. Kamstock D, Elmslie R, Thamm D, Dow S (2007) Evaluation of a xenogeneic VEGF vaccine in dogs with soft tissue sarcoma. *Cancer Immunol Immunother* 56(8):1299–1309.
23. Gavilondo JV, et al.; CENTAURO Group of Investigators (2014) Specific active immunotherapy with a VEGF vaccine in patients with advanced solid tumors. Results of the CENTAURO antigen dose escalation phase I clinical trial. *Vaccine* 32(19):2241–2250.
24. Wang B, Kaumaya PT, Cohn DE (2010) Immunization with synthetic VEGF peptides in ovarian cancer. *Gynecol Oncol* 119(3):564–570.
25. Vicari D, Foy KC, Liotta EM, Kaumaya PT (2011) Engineered conformation-dependent VEGF peptide mimics are effective in inhibiting VEGF signaling pathways. *J Biol Chem* 286(15):13612–13625.
26. Jiang C, Xiong W, Lu BY, Gonda MA, Chang JY (2010) Synthesis and immune response of non-native isomers of vascular endothelial growth factor. *Biochemistry* 49(31):6550–6556.
27. Van Regenmortel MH (2009) What is a B-cell epitope? *Methods Mol Biol* 524:3–20.
28. Christinger HW, et al. (1996) Crystallization of the receptor binding domain of vascular endothelial growth factor. *Proteins* 26(3):353–357.
29. Muller YA, et al. (1998) VEGF and the Fab fragment of a humanized neutralizing antibody: Crystal structure of the complex at 2.4 A resolution and mutational analysis of the interface. *Structure* 6(9):1153–1167.
30. Muller YA, et al. (1997) Vascular endothelial growth factor: Crystal structure and functional mapping of the kinase domain receptor binding site. *Proc Natl Acad Sci USA* 94(14):7192–7197.
31. Mandal K, Kent SB (2011) Total chemical synthesis of biologically active vascular endothelial growth factor. *Angew Chem Int Ed Engl* 50(35):8029–8033.
32. Timmerman P, Beld J, Puijk WC, Meloen RH (2005) Rapid and quantitative cyclization of multiple peptide loops onto synthetic scaffolds for structural mimicry of protein surfaces. *ChemBioChem* 6(5):821–824.
33. Timmerman P, Puijk WC, Meloen RH (2007) Functional reconstruction and synthetic mimicry of a conformational epitope using CLIPS technology. *J Mol Recognit* 20(5):283–299.
34. Liang WC, et al. (2006) Cross-species vascular endothelial growth factor (VEGF)-blocking antibodies completely inhibit the growth of human tumor xenografts and measure the contribution of stromal VEGF. *J Biol Chem* 281(2):951–961.
35. Bagri A, et al. (2010) Effects of anti-VEGF treatment duration on tumor growth, tumor regrowth, and treatment efficacy. *Clin Cancer Res* 16(15):3887–3900.
36. Engelhorn ME, et al. (2006) Autoimmunity and tumor immunity induced by immune responses to mutations in self. *Nat Med* 12(2):198–206.
37. Hsei V, Deguzman GG, Nixon A, Gaudreault J (2002) Complexation of VEGF with bevacizumab decreases VEGF clearance in rats. *Pharm Res* 19(11):1753–1756.
38. Purswani S, Talwar GP (2011) Development of a highly immunogenic recombinant candidate vaccine against human chorionic gonadotropin. *Vaccine* 29(12):2341–2348.
39. Ambühl PM, et al. (2007) A vaccine for hypertension based on virus-like particles: Preclinical efficacy and phase I safety and immunogenicity. *J Hypertens* 25(1):63–72.
40. Singh M, Das SK, Suri S, Singh O, Talwar GP (1998) Regain of fertility and normality of progeny born during below protective threshold antibody titers in women immunized with the HSD-hCG vaccine. *Am J Reprod Immunol* 39(6):395–398.
41. Durez P, et al. (2014) Therapeutic vaccination with TNF-Kinoid in TNF antagonist-resistant rheumatoid arthritis: A phase II randomized, controlled clinical trial. *PLoS One* 9(12):e113465.
42. Simms MS, et al. (2000) Anti-GnRH antibodies can induce castrate levels of testosterone in patients with advanced prostate cancer. *Br J Cancer* 83(4):443–446.
43. Turkstra JA, et al. (2011) Pharmacological and toxicological assessment of a potential GnRH vaccine in young-adult male pigs. *Vaccine* 29(21):3791–3801.
44. Stacker SA, et al. (1999) A mutant form of vascular endothelial growth factor (VEGF) that lacks VEGF receptor-2 activation retains the ability to induce vascular permeability. *J Biol Chem* 274(49):34884–34892.
45. Mäkinen T, et al. (2001) Isolated lymphatic endothelial cells transduce growth, survival and migratory signals via the VEGF-C/D receptor VEGFR-3. *EMBO J* 20(17):4762–4773.
46. Blom AG, Hilgers LA (2004) Sucrose fatty acid sulphate esters as novel vaccine adjuvants: Effect of the chemical composition. *Vaccine* 23(6):743–754.
47. Hilgers LA, Blom AG (2006) Sucrose fatty acid sulphate esters as novel vaccine adjuvant. *Vaccine* 24(Suppl 2):S2-81-2.